Sensors and Actuators B 233 (2016) 566–573

Contents lists available at ScienceDirect

Sensors and Actuators B: Chemical

journal homepage: www.elsevier.com/locate/snb

Thiazole-based ratiometric fluorescence pH probe with large Stokes shift for intracellular imaging

Wen-Jia Zhang[a,1], Li Fan[a,1], Zeng-Bo Li[a], Ting Ou[a], Hua-Jin Zhai[a], Jun Yang[b], Chuan Dong[a], Shao-Min Shuang[a,*]

[a] College of Chemistry and Chemical Engineering, Institute of Environmental Science, Shanxi University, Taiyuan 030006, China
[b] The University of Western Ontario, Department of Mechanical and Materials Engineering, Canada

ARTICLE INFO

Article history:
Received 20 January 2016
Received in revised form 16 April 2016
Accepted 20 April 2016
Available online 23 April 2016

Keywords:
Thiazole-based probe
pH probe
Ratiometric fluorescence
Intracellular imaging
Extreme acidity

ABSTRACT

A ratiometric fluorescent pH probe 4-((1E, 3E)-4-(benzo[d]thiazol-2-yl)buta-1, 3-dienyl)-*N*, *N*-dimethylbenzenamine (**BTDB**) was synthesized via ethylene bridging of thiazol and cinnamaldehyde for extremely acidic sensing. **BTDB** exhibits ratiometric fluorescence emission ($I_{425\,nm}/I_{595\,nm}$) characteristics with pK_a of 2.34 and a large Stokes shift of 177 nm under acidic conditions. The linear response to pH is in the range of 2.3–4.0. Quantum chemical calculations with the B3LYP exchange functional theory demonstrated that the ratiometric response of the probe to acidic pH was due to H^+ binding with the N of cinnamaldehyde and the induced decreases of the intramolecular charger transfer (ICT) process. The as-prepared probe displayed excellent cell membrane permeability was further applied successfully to monitor pH fluctuations in live cells with excellent lysosomal targeting ability, and extreme acidity in *Escherichia coli* cells.

1. Introduction

Intracellular pH plays an indispensable role in a mass of cellular events such as defense enzymatic activity [1], ion transport and homeostasis [2,3]. Intracellular pH also couples to processes such as the cell cycle and apoptosis [4–6]. Maintaining pH homeostasis is fundamental for all living organisms [7–11]. Abnormal pH values can cause cardiopulmonary and neurologic problems including cancer [12] and Alzheimer's disease [13]. Therefore, the accurate measurement of pH changes in live cells is critical for comprehending cellular functions and further understanding physiological and pathological processes.

Fluorescence spectroscopy has attracted much attention over other methods in terms of its excellent sensitivity and convenient operation in many applications. In particular, by combining the use of fluorescent probes and confocal laser scanning microscopy, fluorescent imaging provides a high spatial and temporal resolution for observation of live cells. In order to quantify the pH, the pK_a of the probes needs to match with the pH range of the research system. Nowadays, numerous pH-dependent fluorescent probes with near neutral (pH 6–8) [14–20] or weak acidic (pH 4–6) response behavior [21–30] have been exploited for applications in biological systems. However, relatively less attention was paid on the fluorescent probes with pH sensitive behavior in extremely acidic pH region (pH < 4). Actually most of the living species could hardly live in this strongly acidic conditions, while a mass of microorganisms such as "acidophiles" and Helicobacter pylori particularly favor harsh environments [11,31]. Stomach, which contains gastric acid with acidity pH 2.0–3.0, is the strongly acidic organ of human beings. In the stomach, pepsinogen activated into pepsin by gastric acid [32–34], then the enzyme pepsin digests protein. Also, the extreme acidic environment serves to protect the body from ingested microorganisms by acting as a barrier for bacteria. Abnormal pH values interfere with the function of stomach, which results directly in stomach disorders. Therefore, the precise determination of intracellular pH value under extreme-acidity conditions still faces considerable challenges. Su et. al [35] synthesized the first extremely acidic ratiometric fluorescent probe with the pH response in the range of 1.8–3.4. Yang et al. [36] developed a protein-based pH probe to noninvasively measure the extremely acidic extracellular pH in *Escherichia coli* cells. But up till now, very few pH probes have been applicable for more acidic conditions with pH below 4 [37–39]. Considering the interference from excitation light and complication of cellular system, the development of pH probe with larger Stokes shift for the extreme acidity is desirable.

* Corresponding author.
E-mail address: smshuang@sxu.edu.cn (S.-M. Shuang).
[1] These authors contributed equally to this work.

http://dx.doi.org/10.1016/j.snb.2016.04.122
0925-4005/

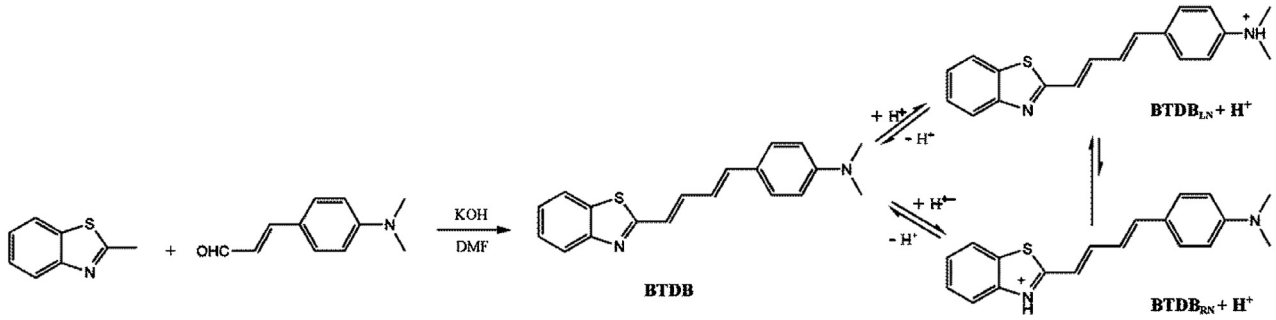

Scheme 1. Synthetic scheme of **BTDB** and its structures in acidic and neutral conditions.

The large Stokes shift can separate the emission and excitation lights well and increase the sensitivity of fluorescence detection, since the possible self-quenching as well as fluorescence detection errors due to the excitation source will be efficiently avoided.

4-((1E,3E)-4-(benzo[d]thiazol-2-yl)buta-1,3-dienyl)-*N*,*N*-dimethylbenzenamine (**BTDB**) (Scheme 1) was widely used as an anti-tumor [40] and anti-HIV active agent [41], and have high non-linear optical effectiveness [42]. From the structure point of view, **BTDB** was ethylene bridged with cinnamaldehyde and benzothiazole, the former can act as an electron donor (D) and the latter can act as an electron acceptor (A). The D-π-A structure type is constantly used as fluorophore to construct intramolecular charge transfer (ICT) fluorescent probes displaying a large Stokes shift. Above thinking induces us to extend the optical behavior and utility of **BTDB**. We found that **BTDB** exhibited pronounced pH-dependent blue-shift properties both in absorption and emission spectra, because protonation significantly decreased the electron-acceptor ability of benzothiazole moiety, and further influenced the D-A interaction with the electron-donating cinnamaldehyde group. Moreover, **BTDB** showed ratiometric fluorescence emission characteristics and large Stokes shift. Additionally, **BTDB** expanded to intracellular imaging under extreme acidity with satisfying results.

2. Experimental

2.1. Materials and apparatus

All reagents and solvents were purchased from commercial sources and used without further purification. 2-Methylbenzothiazole was purchased from Xiya Reagent. 4-(Dimethylamino) cinnamaldehyde was purchased from Aladdin. 3-(4,5-dimethylthiazol-2-yl)-2,5- diphenyltetrazolium bromide (MTT) are commercially available from Thermo-Fisher Biochemical Products (Beijing) Co., Ltd. Nigericin (sodium salt) are obtained from Invitrogen (Carlsbad, CA). All other chemicals were commercially available from Tianjin Fuyu Fine Chemical Co., Ltd.

^{1}H NMR spectra and ^{13}C NMR were recorded on a Bruker 300 MHz NMR spectrometer (Bruker biospin, Switzerland) in the solvent deuterated dimethyl sulfoxide (DMSO-d_6) with tetramethylsilane (TMS) as an internal standard. Mass spectra were acquired with an Agilent Accurate-Mass-Q-TOF MS 6520 system equipped with an electrospray ionization (ESI) source (Agilent, USA). Elemental analyses were obtained on a FLASH EA1112 elemental analysis recorder. Absorption spectra were performed on a HiTAChi U-2910 UV–vis spectrophotometer (Beijing Purkinje General Instrument Co., Ltc., Beijing, China). Fluorescence spectra measurements were taken on an FLS-920 Edinburgh fluorescence spectrophotometer (Edinburgh Co., Ltd.). Fluorescent images were acquired on an FV1000 confocal laser scanning microscope (Olympus Co., Ltd. Japan) with an objective lens (×20). *E. coli* (*E. coli*) cells were incubated in a table concentrator (Shanghai Yiheng Instruments Co., Ltd., China) and centrifuged on a TGL-12GB-C High-speed desktop centrifuge (Shanghai Anting Scientific Instrument Factory, China). Deionized water was obtained from a Milli-Q water purification system (Millipore). pH values were measured with a Beckman Φ 50 pH meter (Shanghai LeiCi Device Works, Shanghai, China).

2.2. Synthesis and characterization of fluorescent probe

The synthetic route of **BTDB** is shown in Scheme 1 [43]. A mixture of 2-Methylbenzothiazole (0.126 mL, 1.0 mmol), 4-(Dimethylamino)cinnamaldehyde (0.263 g, 1.5 mmol) and KOH (0.354 g, 6.25 mmol) in DMF (7 mL) were stirred under N_2 atmosphere for 24 h. After completion, the reaction mixture was filtered to remove KOH. The solvent was removed under reduced pressure and the crude product was purified by column chromatography with methylene chloride/methyl alcohol (20/1, V/V) as eluent to give an orange solid, yield 0.28 g (64%). ^{1}H NMR (300 MHz, DMSO-*d*6) *δ*: 2.961–2.976 (s, 6H), 6.674–6.893 (m, 3H), 6.893–7.032 (d, 2H), 7.290–7.476 (m, 5H), 7.890–8.022 (d, 1H), 8.022–8.047(d, 1H). ^{13}C NMR (300 MHz, DMSO-*d*6) *δ*(ppm): 167.29, 154.11, 151.11, 140.09, 139.37, 134.22, 130.91, 129.08, 128.87, 127.00, 126.88, 125.86, 125.55, 124.69, 124.51, 123.25, 122.64, 122.59, 122.47, 112.64, 112.56, 112.49. MS (ESI-MS): *m*/*z* Calcd 307.1264, found 307.1263 for [M+H]$^+$. Elemental Analysis: Calcd C, 74.47; H, 5.92; N, 9.14, S, 10.46. Found C, 72.98; H, 5.68; N, 9.62, S, 10.05.

2.3. UV–vis and fluorescence titrations

Doubly distilled water is used to prepare all the aqueous solutions. The stock solution of **BTDB** (1.0 mM, ethanol) was diluted to 10.0 μM in ethanol/water (1/2 v/v) medium. In the pH titrations experiments, 2 mL of **BTDB** solutions were poured into a quartz optical cell of 1 cm optical path length each time. Variations in the pH of the solution were adjusted by adding small amounts of HCl (0.25 M, 0.5 M and 1.0 M) or NaOH (0.5 M) and the spectral data are recorded after 2 min for equilibrating each addition. Excitation and emission bandwidths are both set at 2.0 nm, and the excitation wavelengths are 383 nm. All spectroscopic experiments are carried out at 25 °C. The stock solutions of metal ions for selectivity experiments are prepared from their chloride or nitrate salts in doubly distilled water.

2.4. Calculation methods

The calculations in this work were performed with the Gaussian 09 program package. The geometric and electronic structures of molecules were investigated with the density functional theory (DFT) method. In each optimization, the vibrational frequencies were calculated and the results showed that all optimized struc-

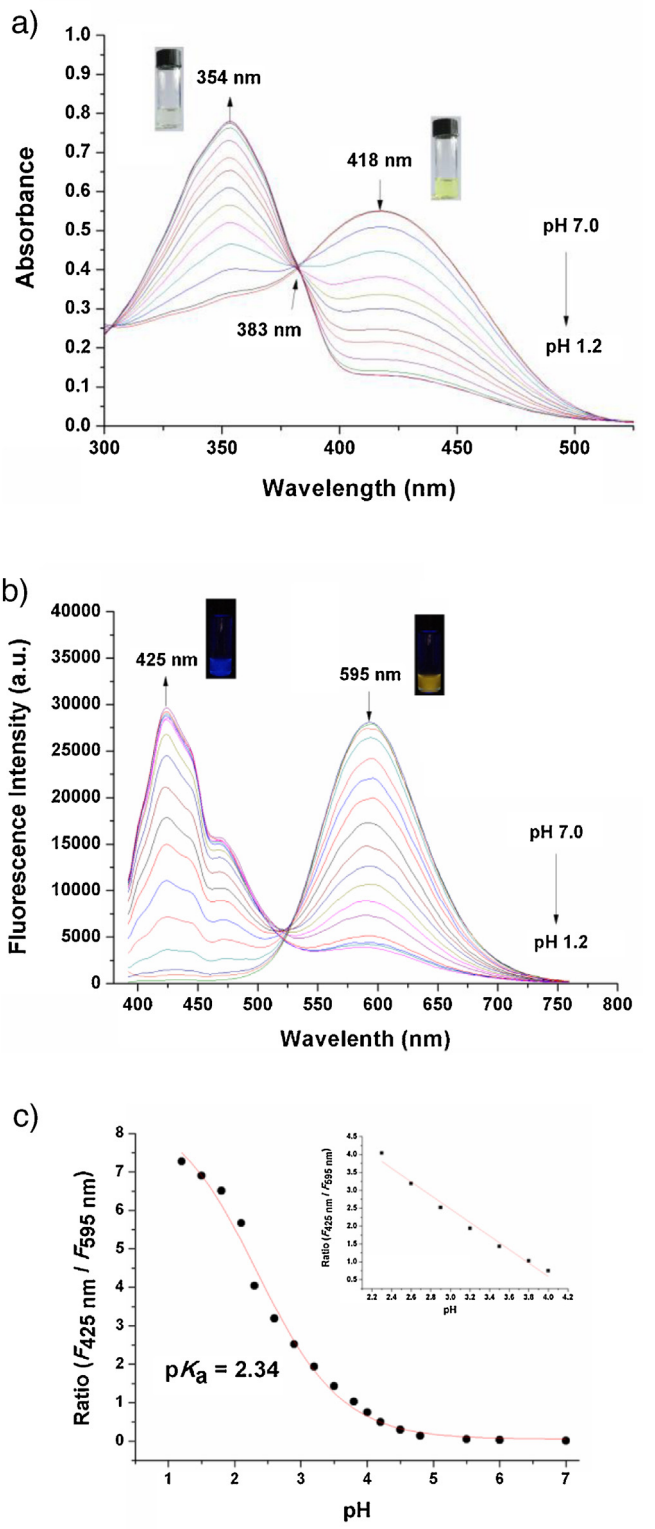

Fig 1. (a) Change of the absorption spectra of **BTDB** with decreasing pH from 7.0 to 1.2. Inset: the color of the solution changed from yellow to colorless with decreasing pH. (b) Change of the fluorescence spectra of **BTDB** with decreasing pH from 7.0 to 1.2 (λex = 383 nm). Inset: The fluorescent color of the solution changed from yellow to blue with decreasing pH. (c) Sigmoidal fitting of the pH-dependent emission (F_{425nm}/F_{595nm}). Inset: the good linearity in the pH range of 2.3–4.0. (For interpretation of the references to colour in this figure legend, the reader is referred to the web version of this article).

tures were stable geometric structures. All DFT calculations were performed using the B3LYP functional and the 6–311 + G (d,p) basis set.

2.5. Cell cytotoxicity assay

According to the literature[44], the MTT assay is used to test the cytotoxicity of **BTDB** on HeLa cells. The cells with a density of 1×10^5 cells mL^{-1} are cultured in a 96-well microplate to a total volume of 200 μL $well^{-1}$ at 37 °C in a 5% CO_2 atmosphere. After 24 h, different concentrations **BTDB** of 0.01 μM, 0.1 μM, 1 μM, 10 μM and 50 μM are incubated with HeLa cells for 3 h in fresh medium, respectively. After washing the cells with cold phosphate buffered saline (PBS, pH 7.4) for 3 times, 10 μL of MTT solution (10 mg/ml, PBS) is added into each well of 96-well microplate for another 4 h. Then the remaining MTT solution is removed from the wells, and 150 μL of DMSO is added into each well to dissolve the intracellular blue-violet formazan crystals. The absorbance of the solution is measured at 490 nm wavelength with a microplate reader. The cell viability is calculated by the following equation:

$$\%\text{viability} = [\sum(A_i/A_{control} \times 100)]/n$$

where A_i is the absorbance of different concentrations probe of 0.01 μM, 0.1 μM, 1 μM, 10 μM and 50 μM, respectively. $A_{control}$ is the average absorbance of the control well in which the probe was absent, and n (=3) is the number of the data points.

2.6. Colocalization experiments

HeLa cells are cultured in DMEM supplemented with 10% FBS, and incubated at 37 °C in a 5% CO2 atmosphere. Cells are seeded on 35 mm diameter round glass Petri dish at a density of 1 × 105 for 24 h. **BTDB** dissolved in DMSO (0.5 μL, 10 mM) are added to the cells medium (500 μL) at 10 μM final concentrations for 10 min, and then cells were washed with PBS three times. 0.1 μM Lyso Tracker Green DND-26 was added and co-incubate for another 30 min and cell imaging was then carried out after washing cells with PBS three times. Then fluorescence images are acquired on an Olympus FV1000 confocal laser scanning microscope with red channel (Ex = 405 nm, Em = 570–620 nm) for **BTDB**; Green channel (Ex = 488 nm, Em = 500–520 nm) for Lyso Tracker DND-26; respectively.

2.7. Culture of HeLa cells for intracellular fluorescent imaging

HeLa cells are cultured in DMEM supplemented with 10% FBS, and incubated at 37 °C in a 5% CO_2 atmosphere. Cells are seeded on 35 mm diameter round glass Petri dish at a density of 1×10^5 for 24 h. **BTDB** dissolved in DMSO (0.5 μL, 10 mM) are added to the cells medium (500 μL) at 10 μM final concentrations for 10 min. Then excess **BTDB** are removed by gentle rinsing with PBS (pH 7.4) for three times and treated with nigericin for additional 10 min in PBS buffer at different pH conditions of 7.4, 4.0 and 3.0, respectively. Then fluorescence images are acquired on an Olympus FV1000 confocal laser scanning microscope with blue channel (Ex = 405 nm, Em = 425–460 nm) and yellow channel (Ex = 405 nm, Em = 570–620 nm), respectively.

2.8. Culture of E. coli cells for intracellular fluorescent imaging

According to the method reported in literature [37], *E. coli* cells are incubated at 37 °C in Luria-Bertani (LB) culture (yeas textract 5 g L^{-1}, Trptone 10 g L^{-1}, NaCl 10 g L^{-1}) in a table concentrator at 180 rpm for 16 h. Then the *E. coli* cells are collected by centrifuging the culture for 5 min at 4500 rpm. The sediment is washed

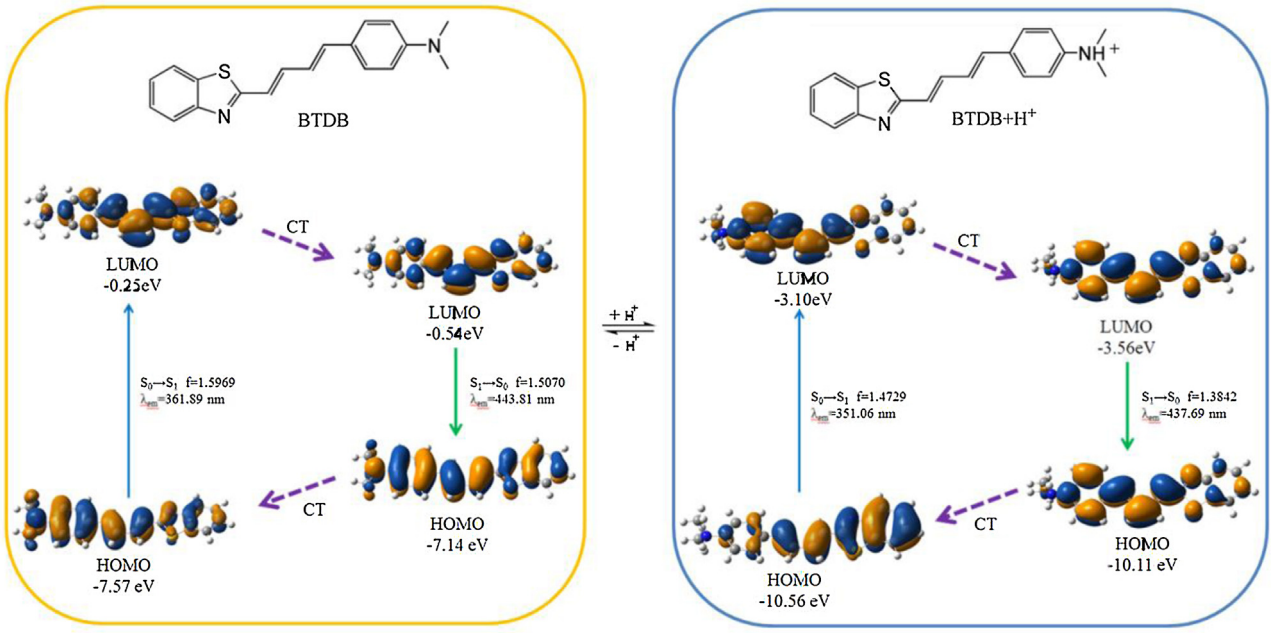

Fig. 2. The frontier molecular orbitals (FMOs) involved in the vertical excitation and emission of **BTDB** and **BTDB** + H^+. CT stands for conformation transformation. Excitation and radiative processes are represented by solid lines and the nonradiative processes by dotted lines.

with sterile water, and then resuspended in different PBS buffers for 5 min at pH 7.0, 4.0, 2.5, 1.2, respectively. **BTDB** dissolved in DMSO is then added into every tube to make the final probe concentration of 10 μM. The **BTDB**-stained *E. coli* cells are incubated in a table concentrator for 2 h. Then they are meared on slides and observed by confocal laser scanning microscope with blue channel (Ex = 405 nm, Em = 425–460 nm) and yellow channel (Ex = 405 nm, Em = 570–620 nm), respectively.

3. Results and discussion

3.1. Spectroscopic properties of *BTDB*

The standard pH titrations of absorption spectra and fluorescence emission spectra were performed. Fig. 1a shows the UV–vis absorption spectra of **BTDB** at varying pH. As the pH decreased from 7.0 to 1.2, the absorption intensity at 418 nm reduced and, concomitantly, a new peak at 354 nm appeared. There is a well-defined isobestic point at 383 nm in the absorption spectra, which can give a good indication that the solutions were of all similar ionic strength and it reduced the influence that other ions might cause on the spectral properties of the probe in relation to protons. The blue shift in the absorption spectra confirms that ICT effect of **BTDB** is reduced with decreasing pH due to the protonation of the dimethylamino moiety (Scheme 1) in the probe. Another observation was a notable color change from yellow to colorless with decreasing pH, which indicated that **BTDB** could serve as a visual probe for the determination of H^+ concentration. Moreover, the molar extinction coefficient is an important parameter for evaluation of a fluorescent probe. According to Fig. 1a, the molar extinction coefficient of **BTDB** could be obtained by use of the Lambert-Beer law in base form, $\varepsilon_1 = 54900\ L\ mol^{-1}\ cm^{-1}$ ($\lambda_{max} = 418$ nm, pH 7.0), and acid form, $\varepsilon_2 = 77553\ L\ mol^{-1}\ cm^{-1}$ ($\lambda_{max} = 354$ nm, pH 1.2).

The pH titration indicates that the probe exhibits remarkable pH-dependent behavior in emission spectra (Fig. 1b). The fluorescence spectrum of **BTDB** at pH 7.0 contains an emission band with a maximum at 595 nm ($\lambda_{ex} = 383$ nm). When the pH was decreased to 1.2, the fluorescence is reduced gradually and the fluorescence emission spectra show a large blue-shift of 170 nm in the emission spectra from 595 nm to 425 nm, which is attributed to the decreased ICT effect. Accordingly, the solution color changes from yellow to blue under irradiation of an UV lamp. The emission ratio (F_{425nm}/F_{595nm}) changes dramatically from 7.27 at pH 7.0–0.05 at pH 1.2 with a huge value change of 145, indicating that **BTDB** is highly sensitive to pH changes (Fig. 1c). What is more important, **BTDB** shows significantly large Stokes shifts of 177 nm under acidic conditions and 71 nm at neutral conditions, respectively, which could help to reduce the excitation interference. These remarked

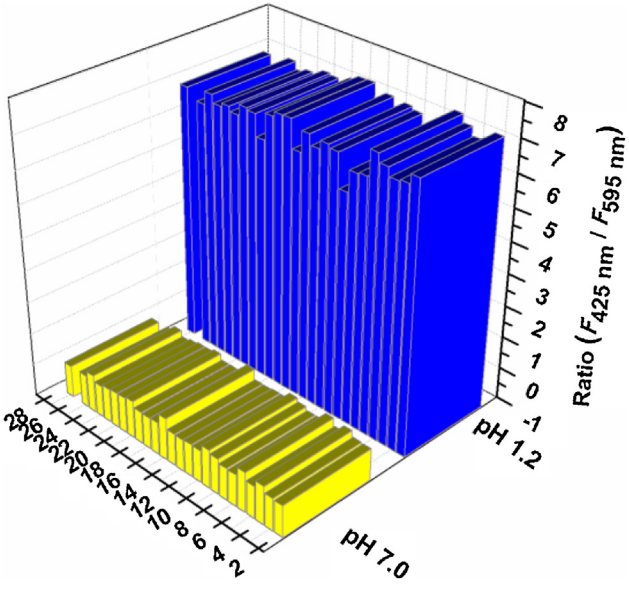

Fig. 3. Fluorescence emission ratio (F_{425nm}/F_{595nm}) of 10 μM **BTDB** in ethanol/water (1/2, V/V) at pH 7.0 and 1.2 in the presence of diverse metal ions: 1, blank; 2, Na^+ (150 mM); 3, K^+ (150 mM); 4, Ca^{2+} (10 mM); 5, Mg^{2+} (2 mM); 6, Co^{2+} (0.2 mM); 7, Cu^{2+} (0.2 mM); 8, Mn^{2+} (0.2 mM); 9, Ni^{2+} (0.2 mM); 10, Ba^{2+} (0.2 mM); 11, Al^{3+} (0.2 mM); 12, Cd^{2+} (0.2 mM); 13, Fe^{3+} (0.2 mM); 14, Pb^{2+} (0.2 mM); 15, Cr^{3+} (0.2 mM); 16, Fe^{2+} (0.2 mM); 17, Zn^{2+} (0.2 mM); glucose (0.2 mM); cysteine (0.2 mM); homocysteine (0.2 mM); glutathione (0.2 mM); arginine (0.2 mM); histidine (0.2 mM); lysine (0.2 mM); vitamin C (0.2 mM)..

changes of emission spectra and fluorescent color provide a good opportunity to achieve ratiometric detection.

Nonlinear fit of the sigmoidal curve (emission intensity ratios (F_{425nm}/F_{595nm}) versus pH value) afforded the probe a pK_a value of 2.34. More interestingly, the fluorescence intensity showed a good linearity with pH in the range of 2.3–4.0 (Fig. 1c), according to the linear equation: $I = 8.16–1.89 \times$ pH with a linear coefficient R^2 of 0.98. These results indicate that **BTDB** could be potentially suitable for monitoring pH variations under the extremely acidic pH environment by ratiometric fluorescence method.

Considering the application of **BTDB** in the living cells, UV–vis and fluorescence titrations were carried out in the presence of 80% cell medium (DMEM) and 20% EtOH as a co-solvent at probes concentration of 10 μM (Fig. S1). The properties of the probe in the presence of cell medium are almost consistent with Fig. 1. It demonstrates that the influences of the cellular environment on the calibration curve were relatively small.

3.2. Theoretical calculations

To better understand the optical responses of **BTDB** upon binding with H^+, we carried out density functional theory (DFT) calculations at the B3LYP/6–311 + G(d) level using Gaussian 09 program. Fig. 2 shows the optimized structure and the lowest unoccupied (LUMO) and the highest occupied molecular orbital (HOMO) plots of the probe and their protonated form.

Protonation of **BTDB** to form **BTDB** $_{LN} + H^+$ and **BTDB** $_{RN} + H^+$ (Scheme 1) under the acidic condition is a competitive process. It is worth noting that the natural bond orbital charge distributions show N1 (−0.480e) with a more negative charge relative to N4 (−0.468e) (Fig. S2), and that the N1 atom should be protonated preferentially, which is in accordance with experiments. As shown in Fig. 2, for both **BTDB** and **BTDB** + H^+, the S_0–S_1 (HOMO–LUMO) transitions are electron density redistributions from the cinnamaldehyde group to the benzothiazole group, which cause ICT occurs in both **BTDB** and **BTDB** + H^+. However, compared with the electron density distribution in the HOMO and LUMO of **BTDB,** with H^+ binding with the N atom of the cinnamaldehyde group, no electron density in the HOMO and LUMO of **BTDB** + H^+ located on the N atom. It indicated that N atom got weakened electron-donating ability, which further decreased the ICT effect. Furthermore, DFT calculations indicate that the HOMO–LUMO energy gap of **BTDB**$_{LN}$ + H^+ (7.46 eV) is significantly higher than that of **BTDB** (7.32 eV), which is coincide with the observation that **BTDB** exhibits a blue shift under acidic condition (Fig. 1).

3.3. Selectivity studies

Considering the complexity of the intracellular environment, an important work of the probe was performed to determine whether other metal ions were potential interferent at pH 7.0 and 1.2, respectively. As shown in Fig. 3, physiologically ubiquitous metal ions such as Na^+, K^+, Ca^{2+} and Mg^{2+} at their physiological concentrations do not give any obvious emission change on pH measurement. Other heavy or transition metal ions, such as Co^{2+}, Cu^{2+}, Mn^{2+}, Ni^{2+}, Ba^{2+}, Al^{3+}, Cd^{2+}, Fe^{3+}, Pb^{2+}, Cr^{3+}, Fe^{2+}, Zn^{2+} also exhibit negligible

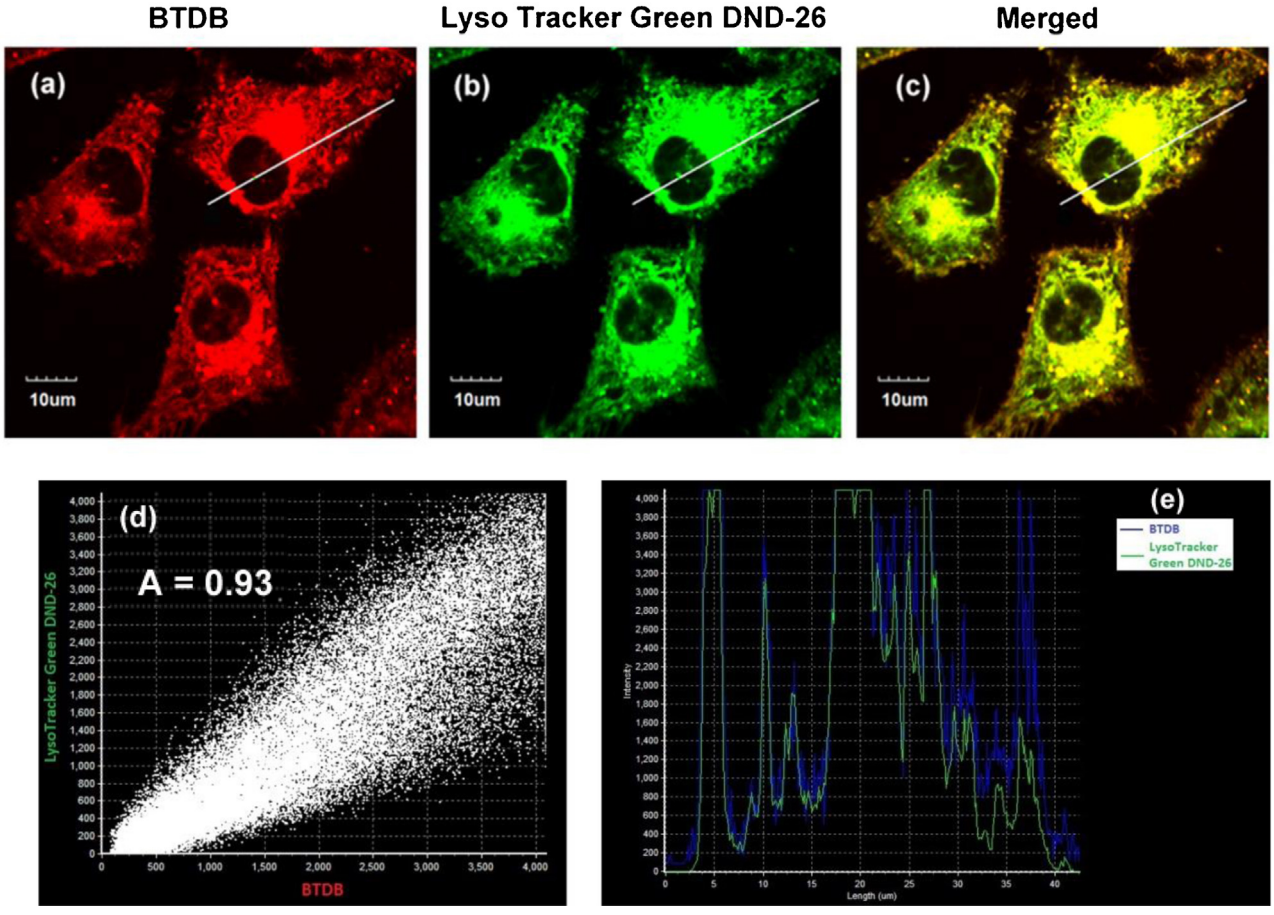

Fig. 4. Pseudo-colour confocal fluorescence image of 10 μM **BTDB** (a) and image of co-labeled with 0.1 μM Lyso Tracker Green DND-26 (b) in HeLa cells. (c) Merged image. (d) The correlation of **BTDB** and Lyso Tracker Green DND-26 intensities (A = 0.93). (e) Intensity profile of linear regions across Hela cells. The fluorescence images are acquired on an Olympus FV1000 confocal laser scanning microscope with red channel (Ex = 405 nm, Em = 570–620 nm) for **BTDB**; Green channel (Ex = 488 nm, Em = 500–520 nm) for Lyso Tracker DND-26; respectively. (For interpretation of the references to colour in this figure legend, the reader is referred to the web version of this article).

effect both under neutral and acidic conditions. Furthermore, some biologically important species (e.g.,) glucose, cysteine, homocysteine, glutathione, arginine, histidine, lysine and vitamin C exhibit negligible effect. These results indicated that **BTDB** shows excellent selectivity to H^+ over representative metal ions.

3.4. Photostability and reversibility studies

It is well-known that photostability is another important parameter to assess the performance of the fluorescent probe. We performed the photostability of **BTDB** by measuring the fluorescent response during 2 h. As shown in Fig. S3, the fluorescence intensity ratios remained stable at pH 1.2, 2.5 and 7.0, respectively, which revealed that **BTDB** could instantly respond to the change of H^+ concentration and our probe can be used to monitor the pH variation in real time.

Since the reversibility is highly required for monitoring reversible pH changes in living organs. Subsequently, the pH value was modulated repeatedly between 1.2 and 7.0 by using concentrated hydrochloric acid and aqueous sodium hydroxide, and the fluorescence intensity ratios of **BTDB** were recorded. As shown in Fig. S4, these processes are fully reversible. Meanwhile, the solution color changed repeatedly between colorless (pH 1.2) and yellow (pH 7.0).

3.5. Cell cytotoxicity assay

Since intracellular acidification has been reported as an early feature of apoptosis in cancer cells, if the probe remaining in the cells induced the cell apoptosis gradually, the pH will be altered to interrupt the measurement. Therefore, MTT assay is crucial to evaluate the cytotoxicity of **BTDB** to live cells. As shown in Fig. S5, more than 87% of cells are viable at various probe concentrations from 0.01 μM to 50 μM, showing the low toxicity of the probe to cultured cells under the experimental conditions of 10 μM.

3.6. Imaging of living cells

Since lysosomes are the typical acidic organelles in cells and **BTDB** could be used for extremely acidic sensing. To demonstrate the lysosomal staining ability of our probe **BTDB**, we conducted co-localization experiments with Lyso Tracker Green DND-26, a well-known green-emissive probe for lysosomes. The image of **BTDB** merged well with the Lyso Tracker Green DND-26 image (Fig. 4a–c). The average Pearson's co-localization coefficient (A) was 0.93 (Fig. 4d). Moreover, the changes in the intensity profile of linear regions of interest (**BTDB** and Lyso Tracker Green DND-26 co-staining) tended toward synchronization (Fig. 4e). There results indicated that **BTDB** has the ability of selective imaging of lysosomes.

In order to explore potential applications in imaging of living cells, the pH-dependent ratiometric emission fluorescence response of **BTDB** in living cells were tested. HeLa cells were firstly incubated with **BTDB** (10 μM) in DMEM medium for 10 min at 37 °C. The cells were washed in PBS buffer at different pH conditions (pH = 7.0, 4.0 and 3.0), and then treated with nigericin for another 10 min, which could quickly equilibrating intracellular and extracellular pH. Fluorescence images were collected on a confocal fluorescence microscope with yellow channel (Ex = 405 nm, Em = 570–620 nm) and blue channel (Ex = 405 nm, Em = 425–460 nm). As shown in Fig. 5, **BTDB** could diffuse into cells and are well dispersed in the whole cytoplasm region, which indicated that **BTDB** had excellent cell membrane permeability. Moreover, it is obvious that the **BTDB**-stained HeLa cells display bright yellow fluorescence (Fig. 5b) and almost no blue fluorescence at pH 7.0 (Fig. 5a). Whereas the living HeLa cells are incubated

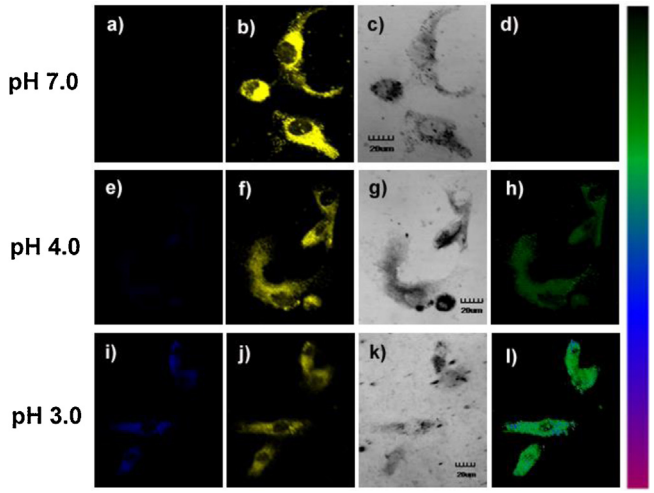

Fig. 5. Fluorescence images of 10 μM **BTDB** in HeLa cells clamped at pH 7.0 (a–d), 4.0 (e–h), 3.0 (i–l). The blue channel images were collected at 425–460 nm (first row, λ_{ex} = 405 nm) and yellow channel images were collected at 570–620 nm (second row, λ_{ex} = 405 nm). The third row shows the corresponding bright-field transmission images. The pseudo ratio images obtained from the blue and yellow channels (fourth row). The bottom color strip represents the pseudocolor change with pH. Scale bar, 20 μm. (For interpretation of the references to colour in this figure legend, the reader is referred to the web version of this article).

with **BTDB** at pH 4.0, a slight quenching in yellow fluorescence (Fig. 5f) and very weak blue fluorescence (Fig. 5e) is observed. Upon the pH are decreased to 3.0, the yellow fluorescence is also decreased (Fig. 5j); by contrast, the blue fluorescence increased significantly (Fig. 5i). Bright-field transmission images confirm the viability of the **BTDB**-stained HeLa cells (Fig. 5c, g and k). In additionally, we obtained the ratio channel based on the blue channel to yellow channel (Fig. 5d, h and l), which display a characteristic pH-dependent signal. These results demonstrate that **BTDB** could be employed for ratiometric imaging of pH fluctuations within the range of pH 7.4–3.0 in living cells.

Although the extreme acidity (pH < 4) is fatal for the majority of living species, a large number of microorganisms including "acidophiles" and Helicobacter pylori have evolved to live under such harsh conditions. Furthermore, some enteric bacteria such as Escherichia coli and Salmonella species can survive through such extreme conditions, causing life-threatening infections. They remains challenging because of the exceeding difficulty in specifically locating small molecule fluorophores in this space [36]. Herein also use confocal laser scanning microscope to visualize the fluorescence change of *E. coli* cells harboring **BTDB** in its periplasmic space. Since the highly permeable outer membrane of *E. coli* cells, its periplasmic pH is quickly equilibrated with the extracellular pH [36]. In order to imaging this periplasmic pH under extreme-acidity conditions, the extracellular pH values were adjusted under various pH values of pH 7.0, 4.0, 2.5 and 1.2, respectively. Similar to **BTDB**-stained HeLa cells, when pH value is higher than 4.0, the *E. coli* cells exhibit the bright yellow fluorescence (Fig. 6a, b) and very weak blue fluorescence emissions (Fig. 6e, f). However, upon the extracellular pH is dropped to 1.2, the yellow fluorescence decreases sharply (Fig. 6c, d) and blue fluorescence increases gradually (Fig. 6g, h). Furthermore, from histogram of fluorescence ratio (F_{blue}/F_{yellow}) versus pH by use of commercial software (Fig. 6m), it is seen that over 125-fold ratio increase is noted with the pH decreasing from 7.0 to 1.2. In particular, a small pH fluctuation surrounding *E. coli* cells under the extreme-acidity condition (pH < 4.0) can give rise to a significant change of fluorescence ratio. The result is perfectly in agreement with the ratiometric emission behavior in Fig. 1c and further confirm that *E. coli* cells could live under such

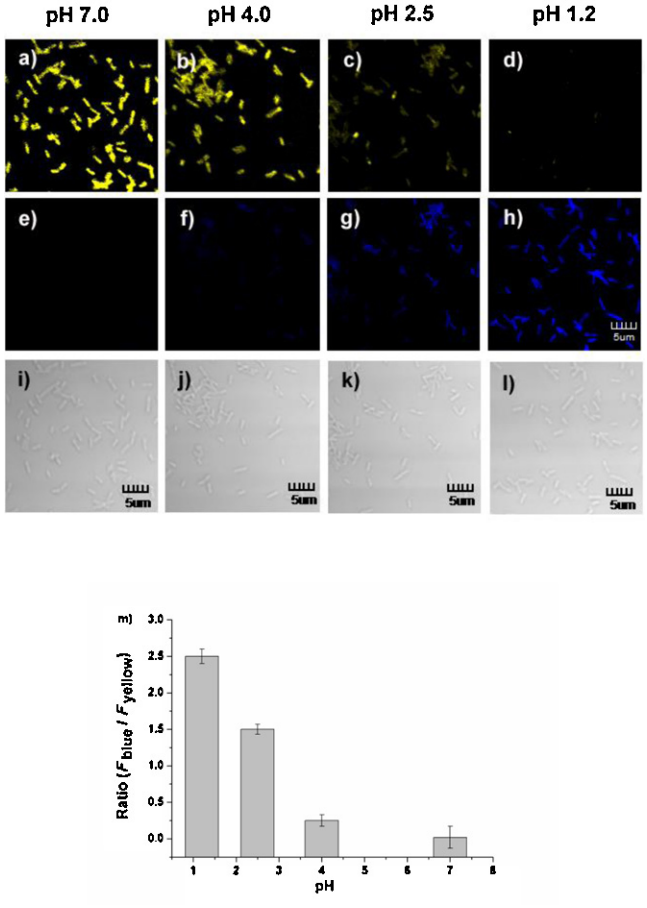

Fig. 6. Fluorescence images of 10 μM **BTDB** in *E. coli* cells clamped at pH 7.0 (a, e and i), 4.0 (b, f and j), 2.5 (c, g and k), pH 1.2 (d, h and l). The yellow channel images were collected at 570–620 nm (first row, λ_{ex} = 405 nm), and blue channel images were collected at 425–460 nm (second row, λ_{ex} = 405 nm). The third row shows the corresponding bright-field transmission images. (m) Intracellular pH calibration curve of **BTDB**. Ratio indicates the pseudo ratio generated by Olympus software. Scale bar, 5 μm. (For interpretation of the references to colour in this figure legend, the reader is referred to the web version of this article).

extremely acidic conditions (i.e. pH 1.2–4.0), which may result in infections. Additionally, our probe **BTDB** is able to monitor such acidic extracellular pH changes in bacteria or other biological systems with characteristic ratiometric emission response.

4. Conclusions

In summary, we have synthesized a thiazole-based ratiometric emission fluorescent probe **BTDB** and its photophysical properties are investigated as a function of pH. This probe exhibits ratiometric response (F_{425nm}/F_{595nm}) to pH and can detect pH changes in the extreme acidity range of 2.3–4.0 with a pK_a of 2.34. It is highly significant that **BTDB** displays a large Stokes shift of 177 nm under acidic conditions, which can reduce the excitation interference. Moreover, other favorable features of **BTDB** include good reversibility, high selectivity, and excellent cell membrane permeability, all of which are favorable for intracellular pH imaging. Application of **BTDB** in Hela cells and *E. coli* cells are also achieved successfully, indicating that **BTDB** can be employed as a ratiometric fluorescent pH probe for imaging pH fluctuations in the physiological pH with excellent lysosomal targeting ability, especially under extreme-acidity condition in bacteria. Thus, it is anticipate for **BTDB** and its derivatives would be potential application for cell imaging in the biomedical and biological fields, and the development of extreme acidic pH probe would also promote biology study on special biological systems.

Aknowledgements

Financial supports from the National Natural Science Foundation of China (No. 21475080 and 21575084), Shanxi Province Hundred Talents Project and Shanxi Scholarship Council of China (No. 2013—key 1). We appreciate Shanxi Medical University (Taiyuan, China) for kindly providing us with the living cells.

Appendix A. Supplementary data

Supplementary data associated with this article can be found, in the online version, at http://dx.doi.org/10.1016/j.snb.2016.04.122.

References

[1] R.T. Kennedy, L. Huang, C.A. Aspenwall, Extracellular pH is required for rapid release of insulin from Zn-insulin precipitates in β-cell secretory vesicles during exocytosis, J. Am. Chem. Soc. 118 (1996) 1795–1796.
[2] K.R. Hoyt, I.J. Reynolds, Alkalinization prolongs recovery from glutamate-induced increases in intracellular Ca^{2+} concentration by enhancing Ca^{2+} efflux through the mitochondrial Na^+/Ca^{2+} exchanger in cultured rat forebrain neurons , J. Neurochem. 7 (1998) 1051–1058.
[3] R.G.W. Anderson, L. Orci, A view of acidic intracellular compartments, J. Cell. Biol. 106 (1988) 539–543.
[4] I.H. Madshus, Regulation of intracellular pH in eukaryotic cells, Biochemical. J. 250 (1988) 1–8.
[5] D. Perez-Sala, D. Collado-Escobar, F. Mollinedo, Intracellular alkalinization suppresses lovastatin-induced apoptosis in HL-60 cells through the inactivation of a pH-dependent endonuclease, J. Biol. Chem. 270 (1995) 6235–6242.
[6] R.A. Gottlieb, J. Nordberg, E. Skowronski, B.M. Babior, Apoptosis induced in Jurkat cells by several agents is preceded by intracellular acidification, Proc. Natl. Acad. Sci. U. S. A. 93 (1996) 654–658.
[7] G. Loving, B. Imperiali, A versatile amino acid analogue of the solvatochromic fluorophore 4-*N*,*N*-dimethylamino-1,8-naphthalimide: a powerful tool for the study of dynamic protein interactions, J. Am. Chem. Soc. 130 (2008) 13630–13638.
[8] G. Loving, B. Imperiali, Thiol-reactive derivatives of the solvatochromic 4-*N*,*N*-dimethylamino-1,8-naphthalimide fluorophore: a highly sensitive toolset for the detection of biomolecular interactions, Bioconjugate Chem. 20 (2009) 2133–2141.
[9] C. Baker-Austin, M. Dopson, Life in acid: pH homeostasis in acidophiles, Trends Microbiol. 15 (2007) 165–171.
[10] J.R. Casey, S. Grinstein, J. Orlowsk, Sensors and regulators of intracellular pH, Nat. Rev. Mol. Cell. Biol. 11 (2010) 50–61.
[11] T.A. Krulwich, G. Sachs, E. Padan, Molecular aspects of bacterial pH sensing and homeostasis, Nat. Rev. Microbiol. 9 (2011) 330–343.
[12] H. Izumi, T. Torigoe, H. Ishiguchi, H. Uramoto, Y. Yoshida, M. Tanabe, I. Tomoko, M. Tadashi, Cellular pH regulators: potentially promising molecular targets for cancer chemotherapy, Cancer Treat. Rev. 29 (2003) 541–549.
[13] T.A. Davies, R.E. Fine, R.J. Johnson, C.A. Levesque, W.H. Rathbun, K.F. Seetoo, S.J. Smith, G. Strohmeier, Non-age related differences in thrombin responses by platelets from male patients with advanced Alzheimer's disease, Biochem. Biophys. Res. Commun. 194 (1993) 537–543.
[14] B. Tang, F.B. Yu, P. Li, L. Tong, X. Duan, T. Xie, X. Wang, A near-infrared neutral pH fluorescent probe for monitoring minor pH changes: imaging in living HepG2 and HL-7702Cells, J. Am. Chem. Soc. 131 (2009) 3016–3023.
[15] J. Han, A. Loudet, R. Barhoumi, R.C. Burghardt, K. Burgess, A ratiometric pH reporter for imaging protein-dye conjugates in living cells, J. Am. Chem. Soc. 131 (2009) 1642–1643.
[16] E. Nakata, Y. Yukimachi, Y. Nazumi, Y. Uto, H. Maezawa, T. Hashimoto, A newly designed cell-permeable SNARF derivative as an effective intracellular pH indicator, Chem. Commun. 46 (2010) 3526–3528.
[17] J. Han, K. Burgess, Fluorescent indicators for intracellular pH, Chem. Rev. 110 (2010) 2709–2728.
[18] U.C. Saha, K. Dhara, B. Chattopadhyay, S.K. Mandal, S. Mondal, S. Sen, A new half-condensed schiff base compound: highly selective and sensitive pH-responsive fluorescent sensor, Org. Lett. 13 (2011) 4510–4513.
[19] L. Fan, Q.L. Liu, D.T. Lu, H.P. Shi, Y.F. Yang, Y.F. Li, C. Dong, S.M. Shuang, A novel far-visible and near-infrared pH probe for monitoring near-neutral physiological pH changes: imaging in live cells, J. Mater. Chem. B 1 (2013) 4281–4288.
[20] L.X. Cao, X.Y. Li, S.Q. Wang, S.Y. Li, Y. Li, G.Q. Yang, A novel nanogel-based fluorescent probe for ratiometric detection of intracellular pH values, Chem. Commun. 50 (2014) 8787–8790.

[21] B. Tang, X. Liu, K.H. Xu, H. Huang, G.W. Yang, L.G. An, A dual near-infrared pH fluorescent probe and its application in imaging of HepG2 cells, Chem. Commun. 36 (2007) 3726–3728.
[22] X.F. Zhou, F.Y. Su, H.G. Lu, P. Senechal-Willis, Y.Q. Tian, R.H. Johnson, D.R. Meldrum, An FRET-based ratiometric chemosensor for in vitro cellularfluorescence analyses of pH, Biomaterials 33 (2012) 171–180.
[23] L. Fan, Y.J. Fu, Q.L. Liu, D.T. Lu, C. Dong, S.M. Shuang, Novel far- visible and near- infrared pH probes based on styrylcyanine for imaging intracellular pH in live cells, Chem. Commun. 48 (2012) 11202–11204.
[24] H. Zhu, J.L. Fan, Q.L. Xu, H.L. Li, J.Y. Wang, P. Gao, X.J. Peng, Imaging of lysosomal pH changes with a fluorescent sensor containing a novel lysosome- locating group, Chem. Commun. 48 (2012) 11766–11768.
[25] G.P. Li, D.J. Zhu, L. Xue, H. Jiang, Quinoline- based fluorescent probe for ratiometric detection of lysosomal pH, Org. Lett. 15 (2013) 5020–5023.
[26] Y.H. Li, Y.J. Wang, S. Yang, Y.R. Zhao, L. Yuan, J. Zheng, R.H. Yang, Hemicyanine-based high resolution ratiometric near-Infrared fluorescent probe for monitoring pH changes in vivo, Anal. Chem. 87 (2015) 2495–2503.
[27] Q.Q. Wang, L.Y. Zhou, L.P. Qiu, D.Q. Lu, Y.X. Wu, X.B. Zhang, An efficient ratiometric fluorescent probe for tracking dynamic changes in lysosomal pH, Analyst 140 (2015) 5563–5569.
[28] Z.Y. Yang, W. Qin, J.W.Y. Lam, S.J. Chen, H.H.Y. Sung, I.D. Williams, B.Z. Tang, Fluorescent pH sensor constructed from a heteroatom-containing luminogen with tunable AIE and ICT characteristics, Chem. Sci. 4 (2013) 3725–3730.
[29] H.S. Lv, J. Liu, J. Zhao, B.X. Zhao, J.Y. Miao, Highly selective and sensitive pH-responsive fluorescent probe in living Hela and HUVEC cells, Sens. Actuators B 177 (2013) 956–963.
[30] R. Sun, X.D. Liu, Z. Xun, J.M. Lu, Y.J. Xu, J.F. Ge, A rosamine-based red-emitting fluorescent sensor for detectingintracellular pH in live cells, Sens. Actuators B 201 (2014) 426–432.
[31] D.S. Merrell, A. Camilli, Acid tolerance of gastrointestinal pathogens, Curr. Opin. Microbiol. 5 (2002) 51–55.
[32] T. Tanaka, R.Y. Yada, Engineered porcine pepsinogen exhibits dominant unimolecular activation, Arch. Biochem. Biophys. 340 (1997) 355–358.
[33] X. Lin, G. Koelsch, J.A. Loy, J. Tang, Rearranging the domains of pepsinogen, Protein. Sci. 4 (1995) 159–166.
[34] X.L. Lin, R.N. Wong, J. Tang, Synthesis purification, and active site mutagenesis of recombinant porcine pepsinogen, J. Biol. Chem. 264 (1989) 4482–4489.
[35] M.H. Su, Y. Liu, H.M. Ma, Q.L. Ma, Z.H. Wang, J.L. Yan, M.X. Wang, 1,9-Dihydro-3-phenyl-4H-pyrazolo[3,4-b]quinolin-4-one, a novel fluorescent probe for extreme pH measurement, Chem. Commun. 11 (2001) 960–961.
[36] M.Y. Yang, Y.Q. Song, M. Zhang, S.X. Lin, Z.Y. Hao, Y. Liang, D.M. Zhang, P.R. Chen, Converting a solvatochromic fluorophore into a protein- based pH indicator for extreme acidity, Angew. Chem. Int. Ed. 51 (2012) 7674–7679.
[37] Y. Xu, Z. Jiang, Y. Xiao, F.Z. Bi, J.Y. Miao, B.X. Zhao, A new fluorescent pH probe for extremely acidic conditions, Anal. Chim. Acta 820 (2014) 146–151.
[38] W.F. Niu, L. Fan, M. Nan, Z.B. Li, D.T. Lu, M.S. Wong, S.M. Shuang, C. Dong, Ratiometric emission fluorescent pH probe for imaging of living cells in extreme acidity, Anal. Chem. 87 (2015) 2788–2793.
[39] M. Nan, W.F. Niu, L. Fan, W.J. Lu, S.M. Shuang, C.Z. Li, C. Dong, Indole-based pH probe with ratiometric fluorescence behavior for intracellular imaging, RSC Adv. 5 (2015) 99739–99744.
[40] M. Kawakami, K. Koya, T. Ukai, N. Tatsuta, A. Ikegawa, K. Gawa, et al., Structure- activity of novel rhodacyanine dyes as antitumor agents, J. Med. Chem. 41 (1998) 130–142.
[41] R. Garg, S.P. Gupta, 2,2′-Dithiobisbenzamides derived from α-, β- and γ-amino acids possessing anti-HIV activities: synthesis and structure ± activity relationship, Bioorg. Med. Chem. 6 (1998) 1707–1730.
[42] P. Hrobarik, P. Zahradink, W.M.F. Fabian, Computational design of benzothiazole- derived push- pull dyes with high molecular quadratic hyperpolarizabilities, Phys. Chem. Chem. Phys. 6 (2004) 495–502.
[43] S.E.H. Etaiw, T.A. Fayed, N.Z. Saleh, Photophysics of benzazole derived push–pull butadienes: a highly sensitive fluorescence probes, J. Photochem. Photobiol. A: Chem. 177 (2006) 238–247.
[44] P.S. Song, X.T. Chen, Y. Xiang, L. Huang, Z.Y. Zhou, R.R. Wei, A.J. Tong, Aratiometric fluorescent pH probe based on aggregation-induced emission enhancement and its application in live-cell imaging, J. Mater. Chem. 21 (2011) 13470–13475.

Biographies

Wenjia Zhang received her BSc degree in chemistry from Shanxi University. She is currently pursuing her MSc degree at Shanxi University and major in analytical chemistry.

Li Fan received her MSc degree in inorganic chemistry in 2006, and PhD degree in analytical chemistry in 2014 from Shanxi University. She is currently a lecturer in Institute of Environmental Science, Shanxi University. Her research focuses on the development of novel fluorescent probe for intracellular imaging.

Zengbo Li received his BSc degree in microbiology in 2006 from Northwest A&F University. He is currently pursuing his PhD degree at Shanxi University and major in biochemical analysis.

Ting Ou received her BSc degree in chemistry from Shanxi University. She is currently pursuing her MSc degree at Shanxi University and major in material chemistry.

Huajin Zhai is a professor of material chemistry at Shanxi University. He received his BSc degree in chemistry and MSc degree in 1990 and 1993 from Wuhan University, respectively, and PhD degree in 1998 from Chinese Academy of Sciences. He has published over 110 SCI papers and he research interests are in the areas of physical chemistry, material chemistry and Nanoclusters.

Jun Yang is a professor of Mechanical and Materials Engineering at Western University. He has published over 60 papers and he research interests are in the areas of biomedicine, nanometer materials and 3D printing.

Chuan Dong is a professor of analytical chemistry in Institute of Environmental Science, Shanxi University. He received his BSc degree in chemistry and MSc degree in analytical chemistry in 1984 and 1990, respectively, and PhD degree in 2002 from Shanxi University. He has published extensively in journals such as Nanoscale, Biosensors and Bioelectronics, Journal of Materials Chemistry B, Chemical Communications, Sensors and Actuators B, Analytical Chemistry, Talanta, etc. His current research interests are biosensors, chemosensors, opticalfiber sensor, fluorescence and room temperature phosphorescence, and environ-mental analysis and monitoring.

Shaomin Shuang is a professor of analytical chemistry at Shanxi University. She received her BSc degree in chemistry and MSc degree in analytical chemistry in 1986 and 1989 from Shanxi University, respectively, and PhD degree in 1998 from South China University of Technology. She has published over 200 papers and her research interests are in the areas of analytical chemistry, super-molecular chemsitry, and photochemsity.